Interfacial oxidation and photoluminescence of InP-Based core/shell quantum dots

Article

Interfacial Oxidation and the Photoluminescence of InP-Based Core/Shell Quantum Dots

Mickael D. Tessier, Edwin A. Baquero, Dorian Dupont, Valeriia Grigel, Eva Bladt, Sara Bals, Yannick Coppel, Zeger Hens, Céline Nayral, and Fabien Delpech

Chem. Mater., **Just Accepted Manuscript** • DOI: 10.1021/acs.chemmater.8b03117 • Publication Date (Web): 12 Sep 2018

Interfacial Oxidation and the Photoluminescence of InP-Based Core/Shell Quantum Dots

Mickael D. Tessier,[*,1,2,‡] Edwin A. Baquero,[3,4,‡] Dorian Dupont,[1,2] Valeriia Grigel,[1] Eva Bladt,[5] Sara Bals,[5] Yannick Coppel,[6] Zeger Hens,[1] Céline Nayral,[3] Fabien Delpech[*,3]

[1]Physics and Chemistry of Nanostructures and Center for Nano and Biophotonics, Ghent University, Ghent, Belgium.

[2]SIM vzw, Technologiepark 935, BE-9052 Zwijnaarde, Belgium

[3]Université de Toulouse, INSA, UPS, CNRS, Laboratoire de Physique et Chimie des Nano-Objets, Toulouse, France.

[4]Departamento de Química, Facultad de Ciencias, Universidad Nacional de Colombia, Sede Bogotá, 111321 Bogotá, Colombia.

[5]Electron Microscopy for Materials Science (EMAT), University of Antwerp, Groenenborgerlaan 171, 2020 Antwerp, Belgium

[6]Laboratoire de Chimie de Coordination, CNRS, UPR 8241, Université de Toulouse, Toulouse, France.

ABSTRACT: Indium phosphide colloidal quantum dots are emerging as an efficient cadmium-free alternative for opto-electronic applications. Recently, syntheses based on easy-to-implement aminophosphine precursors have been developed. We show by solid-state nuclear magnetic resonance spectroscopy that this new approach allows oxide-free indium phosphide core or core/shell quantum dots to be made. Importantly the oxide-free core/shell interface does not help to obtain higher luminescent efficiencies. We demonstrate that in the case of InP/ZnS and InP/ZnSe, a more pronounced oxidation concurs with a higher photoluminescence efficiency. This study suggests that a II-VI shell on a III-V core generates an interface prone to defect. The most efficient InP/ZnS or InP/ZnSe QDs are therefore made with an oxide buffer layer between the core and the shell: it passivates these interface defects but also results in a somewhat broader emission linewidth.

Colloidal quantum dots (QDs) are enabling materials for a variety of luminescence-related applications[1] and, since 2013, products that contain QDs have appeared on the market.[2] In general, however, the requirements of this emerging QD technology with respect to QD synthesis and properties are very different from what academic QD research has provided during the past 30 years. In particular, toxicity, cost, ease of manufacturing and performance are crucial criteria to meet technology requirements. In this context, indium phosphide (InP) QDs are excellent candidates to bring QD science and technology together as these QDs are less toxic, and consequently less restricted, than the widely studied cadmium-based QDs.[3] This economic perspective has inspired the recent development of protocols that use aminophosphines, a cheap and easy-to-use phosphorus precursor, to produce InP QDs with state-of-the-art emission characteristics.[4–8] Even so, differences remain with Cd-based QDs. For example, whereas the photoluminescence quantum yield (PLQY) of Cd-based QDs can reach 90-100 %,[9,10] a PLQY of 70 % at best is more typical of InP-based QDs.[11–13] Understanding the factors that limit the luminescence efficiency remains therefore an essential step to further the technological relevance of InP QDs.

In contrast to CdSe, InP is highly oxophilic, which makes that InP QDs are prone to oxidation, in particular when exposed to water.[14] Water-induced oxidation is especially important in the case of the most widely used route to InP QDs, in which indium carboxylates are used as the indium precursor.[3,11,15–17] It has been shown that indium carboxylates can form water *in situ* either by a ketonisation reaction,[14] or by an amidation reaction when an alkylamine is used as an additional ligand.[18] The general effect of water, which could also come from hydrated indium precursors, solvent or ligands, is the formation of a phosphate layer at the surface of the InP QDs.[14,19] This oxide layer has a direct influence on the synthesis as it blocks the nanocrystals growth,[19] lowers the reaction chemical yield,[20] and modifies the optical properties. The two main phosphorus precursors used to make InP QDs are currently tris-trimethylsilylphosphine [$(TMS)_3P$] and aminophosphines such as tris-diethylaminophosphine or tris-dimethylaminophosphine.[3–7,11,13,16,20,21] While the first is almost always combined with indium carboxylates, an inherent source of water,[14] the second is combined with indium halides and other oxygen-free and water-free compounds. It is therefore possible to make oxide-free InP QDs using the aminophosphine route.[20]

Here, we report on the relation between oxidation and the optical properties of InP/ZnS and InP/ZnSe QDs, starting from InP core QDs synthesized using tris-diethylaminophosphine. Importantly, the samples studied shared the same InP core QDs but were oxidized to a different degree during shell growth. For each sample, the degree of oxidation was quantified using solid-state nuclear magnetic resonance spectroscopy (solid-state NMR) and the key photoluminescence descriptors, i.e., peak emission wavelength, linewidth and PLQY were determined. We demonstrate that oxide-free core/shell InP/ZnS or InP/ZnSe QDs can be obtained by a shell growth

protocol that avoids zinc carboxylates. This model system consists of a pure III-V core (InP) coated by a pure II-VI shell (ZnS or ZnSe). Interestingly, we find that suppressing InP oxidation results in core/shell QDs with a deteriorated photoluminescence efficiency. On the other hand, we show that the formation of ZnS or ZnSe shells by means of zinc carboxylate precursors induces oxidation of the InP at the core/shell interface. The oxidized samples exhibit a higher PLQY and a somewhat broader emission linewidth.

Results.

Oxide-free InP core. We synthesized InP QDs by reacting tris-diethylaminophosphine (DEAP) and indium trichloride in oleylamine in the presence of zinc chloride using the now well-established aminophosphine chemistry.[4–6,20,21] InP QDs with a diameter of (3.2 ± 0.4) nm nm are obtained when indium chloride and zinc chloride are used (see Transmission Electron Microscopy TEM image in Figure S1, Supporting Information).[5] As shown in Figure 1a, this concurs with an excitonic feature at 560-570 nm. As shown before, solid state NMR is most useful to study InP oxidation as it can be used to distinguish between InP and $InPO_X$ (x=2-4) and quantify the fraction of oxidized phosphorous.[14] In Figure 1b, a MAS ^{31}P NMR spectrum of an InP QDs powder, obtained using an oxygen-free purification and drying procedure (see experimental section in Supporting Information for details), is shown. As indicated in Figure 1b, the resonance at -200 ppm corresponds to phosphorous present in nanocrystalline InP.[14] Additionally, a small peak at 6 ppm, that is enhanced in the ^{1}H-^{31}P Cross-Polarization (CP) MAS NMR spectrum of the same sample (see Figure 1c), corresponds to $InPO_4$ that is present on the surface.[14] We can evaluate the percentage of oxidation by comparing the area of the resonances assigned to InP and $InPO_4$ respectively. As we have recently demonstrated, this $^{31}PO_4$ phosphate signal results from the overlap of the resonances of several phosphate species: $O=P(OM)_x(OH)_{3-x}$ (M=In, x=1-3).[22] For the example shown in Figure 1b, this yielded only 2% of oxidized phosphorous. This result confirms previous studies that showed that the aminophosphine-based protocol allows oxide-free InP QDs to be made, thanks to the use of water-and carboxylate-free precursors.[20,21] The minor residual oxidation we observe probably results from the postsynthetic treatment as already underlined by Buffard et al.[21] It should be noted that InP QD synthesized using aminophosphines are not luminescent, which points towards the presence of surface traps. Last, two minor resonances appear at 80 ppm in the ^{31}P spectrum and at 60 ppm in the ^{1}H-^{31}P CP spectrum. The first one has already been observed in the same type of synthesis but has not been attributed yet.[21]

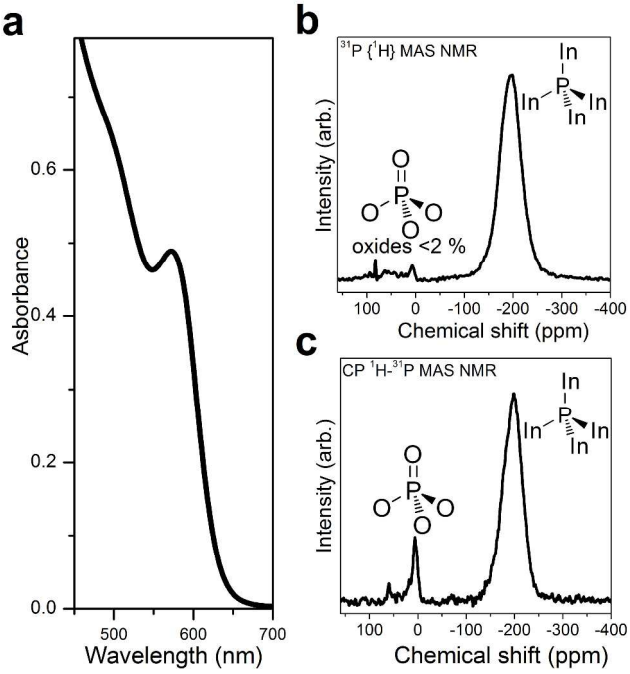

Figure 1: **a.** Absorption spectrum of InP QDs solution. **b.** ^{31}P (spinning speed 16 kHz) and **c.** ^{1}H-^{31}P CP MAS solid-state NMR of InP QDs (spinning speed 18 kHz).

Evidence of the presence of oleylamine as the stabilizing organic ligand at the QD surface is provided by the ^{1}H Magic Angle Spinning (MAS) spectrum (Figure 2a). Resonance signals were found at 5.37, 2.06, 1.34, and 0.93 ppm that are respectively attributed to the alkene protons, the CH2 adjacent to the double bound, the alkane CH2 groups and the CH3 group.[23] The α-CH_2 protons adjacent to the NH_2 group display a broad resonance at 2.9 ppm.[23] The peak at 0.1 ppm corresponds to the vacuum grease used during the synthesis. In the ^{1}H-^{13}C CP MAS NMR spectrum, the alkene resonance appears at δ 129 ppm, while the alpha-CH_2, and the remaining 14 CH_2 groups of oleylamine at δ 42 and 31-27 ppm, respectively (Figure S2). The signals of the methyl group and of the neighbor methylene are barely visible at δ 14 ppm and 22 ppm, respectively. The intensity of the α-CH_2 resonance is significantly decreased in the ^{13}C Direct Polarization (DP) spectrum (Figure S2), an effect of long relaxation times that are due to the ligand rigidity at the QD surface. In contrast, the signal intensity of both the alkene and the terminal methylene as well as the methyl groups are enhanced due to their increased mobility. A Rutherford backscattering (RBS) spectrum, recorded on a thin film of as synthesized, purified InP QDs is represented in Figure 2b. It can be seen that the spectrum features 4 signals, which correspond to backscattering on P, Cl, Zn and In nuclei. From the integrated signal intensity, we estimate the atomic composition of the core InP QDs as 41 % of In, 37 % of P, 16 % of Cl and 5 % of Zn. Focusing first on In and P, the elements constituting the actual inorganic core QDs, we thus find an In/P ratio of approximately 1.1. In line with several metal chalcogenide nanocrystals, such as CdSe, CdTe, PbS and PbSe, we thus find that the InP nanocrystal is enriched in cations (indium in this case) which are probably present as a surface excess. In addition, the RBS spectrum indicates that a purified InP nanocrystal sample also contains Zn and Cl. We

know from Raman spectroscopy that Zn is most likely not incorporated into the InP core,[24] suggesting that the InP nanocrystals have a surface enriched in Zn. The charge on the excess surface cations (both In^{3+} and Zn^{2+} in this case) must be compensated by anions. In the case of CdSe nanocrystals synthesized in the presence of carboxylic acids, these anions typically involve carboxylates that bind as X-type ligands to the nanocrystal surface. Here, on the other hand, we find that 16 % of Cl is present, which nearly compensate the charge on the excess In and Zn. This indicates that the InP surface can be best seen as terminated by an excess of $InCl_3$ and $ZnCl_2$, which makes for overall charge neutral nanocrystals (Figure 2b, inset).

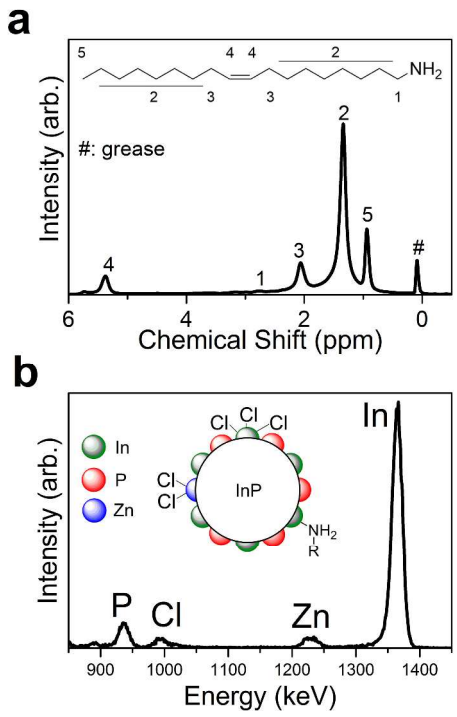

Figure 2: a. ^{1}H MAS NMR spectrum (spinning speed 18 kHz). and **b.** RBS spectrum of oxide-free InP QDs core. Inset: schematic representation of the surface chemistry of InP QDs.

Oxide-free core/shell InP-based QDs.

In order to prevent InP oxidation during shell growth, we developed a shelling protocol involving trioctylphosphine, sulfide or selenide, and zinc chloride dispersed in degassed oleylamine thus avoiding any trace of carboxylates (see Experimental Section in Supporting Information for details). We have first synthesized InP/ZnS which attained a size of (3.7 ± 0.3) nm by this method (Figure S3). As expected, oleylamine was found to be the stabilizing organic ligand according to the ^{1}H MAS and ^{13}C DP MAS experiments (Figures S4 and S5, respectively). The MAS ^{31}P NMR spectrum of this sample is presented in Figure 3a. While the InP resonance signal is clearly visible, the resonance of the oxidized species ($InPO_4$ and $InPO_3$) are barely detected and the fraction of oxidation is largely identical to the InP core QDs. This demonstrates that the use of carboxylate-free shell precursors can effectively suppress oxidation at the core/shell interface. We also synthesized (7.7 ± 1.1) nm InP/ZnSe QDs following by a similar protocol (see Experimental Section and Figure S6 in Supporting Information for details). The corresponding ^{31}P MAS NMR spectrum, which confirms an oxide-free core/shell structure, is presented in Figure 3b. Besides the phosphide and phosphate resonances at -191 and 5 ppm respectively, one can observe some residual free TOPO (56 ppm) and $[P(NHR)_4]Cl$ (31 ppm) in the zinc chloride-based shelling. It has been demonstrated that InP QDs have a strong tendency to oxidize.[14,25,26] Consequently the fact that oxide-free core/shell InP-based QDs can be made is not a minor feat that has to the best of our knowledge was only demonstrated using tris(N,N'-diisopropylacetamidinato)indium(III) as an indium precursor and *via* assisted H_2 growth or low temperature (150 °C) synthesis.[18] In Figures 3c and 3d, we present the photoluminescence spectra of the obtained samples. The InP/ZnS presents an emission full width at half maximum (FWHM) of 50 nm and a PLQY of only 4 %. While the FWHM is narrower than what is typically obtained for InP/ZnS,[5] the PLQY is considerably lower. Likewise, the oxide-free InP/ZnSe QDs exhibit a lower PLQY as compare to state-of-the-art InP/ZnSe.[5] We have recently demonstrated that the Raman spectra of core/shell InP/ZnSe QDs synthesized using DEAP feature separate InP and ZnSe Raman lines, which points that a neat InP/ZnSe core/shell system is formed, rather than an InZnP core surrounded by a pure ZnSe shell.[24] Here, we show that such a heterostructure can be made with an oxide-free III-V/II-VI core/shell interface. We performed XRD and a high resolution high angle annular dark field scanning transmission electron microscopy (HAADF-STEM) investigation which clearly show the formation of crystalline ZnSe shell (Figure S7 and S8). However, low PLQY are measured which can imply the presence of defects at the interface. III-V/II-VI heterointerfaces grown by molecular beam epitaxy have been studied in the literature, mostly using the nearly strain free GaAs/ZnSe system as an example. Focusing in first instance on the abrupt interface, a point that is made in the literature is that the GaAs/ZnSe boundary can be made either through Ga-Se or As-Zn contacts.[27] Compensation is possible through mixed interfaces that involve, for example, mixed (Ga,Zn) or (As,Se) planes,[28] or vacancies.[29] Importantly, the atomistic structure of the interface has a huge impact on band offsets, and can lead to a density of states with metallic character.[28,29] The I-V characteristics of GaAs/ZnSe junctions were shown to be strongly dependent on the growth conditions, and trapping at the GaAs/ZnSe interface could be demonstrated using Raman scattering.[30] Opposite from a flat interface, a unique interfacial composition will be difficult to accomplish in the case of nanocrystals. The InP core, for example, can expose both In-rich and P-rich (111) surfaces or tend to balance donor and acceptor bonds at (100) surfaces. From this perspective, the chemical heterogeneity of the III-V/II-VI interface could be an intrinsic cause of interfacial trap states that accounts for the low PLQY of oxide-free InP/ZnS and InP/ZnSe QDs.

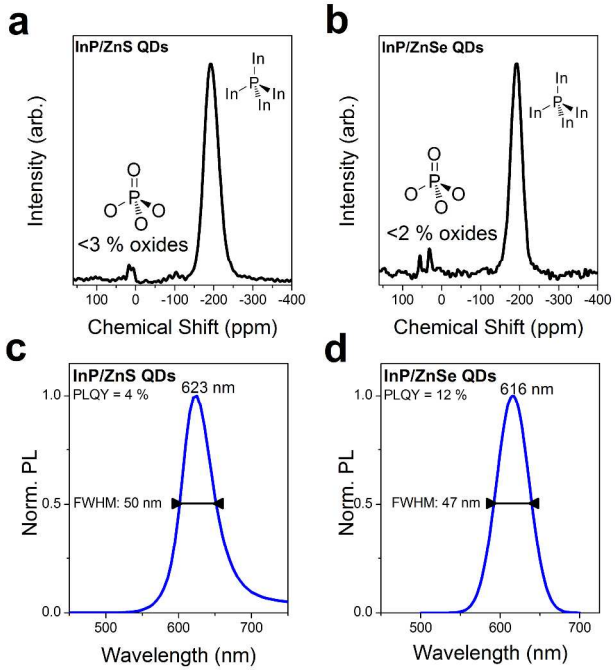

Figure 3: InP/ZnS QDs and InP/ZnSe synthesized using zinc chloride dispersed in oleylamine. **a.** and **b.** ^{31}P MAS spectrum (spinning speed 16 kHz for InP/ZnS and 12 kHz for InP/ZnSe). **c.** and **d.** photoluminescence spectra

Oxidized core/shell InP-based QDs

A second approach we followed for growing a ZnS or ZnSe QDs shell made use of trioctylphosphine sulfide and zinc stearate dispersed in octadecene as precursors.[5] Zinc stearate was prepared in air and degassed thoroughly before use. TEM images of the thus obtained InP/ZnS and InP/ZnSe QDs are shown in the supporting information (Figure S9 and S10). A MAS ^{31}P NMR spectrum of the InP/ZnS QDs sample is presented in Figure 4. In this case, the resonances of both InP and $InPO_4$ can be clearly observed. For InP/ZnS, 60 % of the phosphorus atoms are present as phosphate. The increased intensity of the PO_4 resonance in the ^{1}H-^{31}P CP MAS NMR spectrum clearly demonstrates that the oxide is located at the core/shell interface (Figure S11). A more detailed description of this interface results from a ^{1}H Forth and Back Cross Polarization (FBCP) MAS NMR experiment.[22] Such a measurement relies on the transfer of polarization from H atoms that are part of the stabilizing ligand to the P atoms at the QD and back to the closest H atom. In this way, we can detect P-OH species that are usually invisible with the classical ^{1}H MAS NMR techniques. The ^{1}H/^{31}P FBCP spectrum clearly shows two different P-OH species at δ 8.34 and 6.27 ppm that are not detected in the ^{1}H MAS spectrum (Figure S12). They can be assigned to the acidic phosphate protons P–O–H of HPO_4^{2-} (or $H_2PO_4^-$) moieties as previously observed with calcium phosphates.[31,32] The broadness, and the difference in chemical shifts of these two resonances is a consequence of different hydrogen bonded environments (the stronger the hydrogen-bond, the higher the chemical shift).[31,32] This interpretation was further confirmed by the presence of a correlation cross-peak between these hydroxyl moieties and the phosphorous signals in the 2D ^{1}H-^{31}P Heteronuclear Correlation (HETCOR) MAS NMR spectrum (Figure S13). Consistently with the InP core,[22] this shows that the phosphate species that exist at the interface are manifold: $O=P(OM)_x(OH)_{3-x}$ (M= In and/or Zn; x=1-3) species. These different species cannot be discriminated and the phosphate $^{31}PO_4$ signal at ~5 ppm thus, results from the overlap of the resonances of all the ^{31}P tetraoxophosphorus (V) fragment. Clearly, growing a ZnS shell by means of trioctylphosphine sulfide and zinc stearate results in the oxidation of the InP surface. Given the core diameter of 3.2 nm,[5] we estimate that around 50 % of the P atoms are at the surface.[33] Therefore, we consider that one monolayer of InP has been oxidized. We also used zinc stearate prepared under anhydrous conditions in order to remove the water impurity to make similar InP/ZnS QDs. The obtained sample was also oxidized as the ^{31}P MAS NMR spectrum reveals (51 % oxides, Figure S14) and have a similar size with the other InP/ZnS samples (3.5 nm, Figure S15). This result clearly shows that oxidation is inherently due to the carboxylate precursors as it has been observed previously both in the $(TMS)_3P$-based synthesis and in the subsequent shelling.[14,34] We have also grown a crystalline ZnSe shell using zinc stearate and trioctylphosphine selenide (see XRD and HAADF-STEM in Figure S7 and S16). Likewise the phosphate resonance in the MAS ^{31}P NMR (Figure S17) is observed and from its intensity, we find that 58% of the phosphorous is oxidized. In this case, we also observe the presence of a new and intense resonance at -7 ppm which can be assigned to TOPO interacting with the surface as reported by Tomaselli et al.[35] Indeed, when zinc stearate is used as a zinc source, TOPO appears during the shell growth process (Figure S18) while with zinc chloride this amount is marginal (Figure S19).

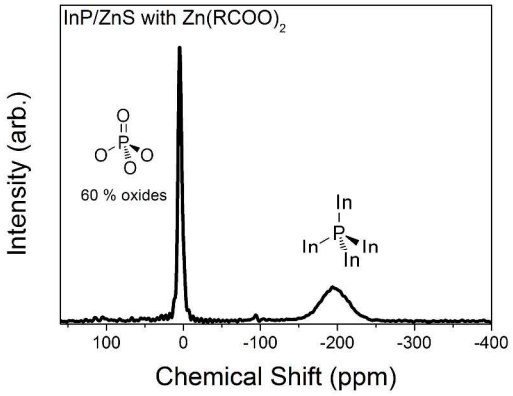

Figure 4: ^{31}P MAS spectrum (spinning speed 16 kHz) of InP/ZnS QDs synthesized using zinc stearate.

Discussion

The different InP/ZnS and InP/ZnSe samples studied here used identical InP core size, which makes that these samples provide fully comparative data. In Table 1, we summarize the photoluminescence and structural data of the different analyzed samples. A first surprise outcome of this comparison is that in spite of a strong difference in the percentage of oxidation between the samples prepared with zinc stearate and zinc chloride (both for ZnS and ZnSe shells), they emit at the same wavelength. For instance, in the case of InP/ZnS samples, one monolayer of the InP core is oxidized. This suggests that the effective InP core diameter is smaller in the oxidized sample

(diameter <2.6 nm: 3.2 nm minus at least one oxidized monolayer) than in the non-oxidized sample (diameter = 3.2 nm). A change of the effective InP core diameter should imply a change in the quantum confinement of the charge carriers and, consequently, a change of the emission wavelength. This is not what we find. This situation somewhat resembles the shift in the band-gap when a semiconductor nanocrystal is grown larger by colloidal atomic layer deposition. Both in the case of CdS or CdSe shell growth around PbS or HgSe, a change in bandgap is only observed when the anion layer is grown, not when the cations are deposited.[36,37] Importantly, for InP QDs it has also been demonstrated that cadmium carboxylates adsorption do not change the QD bandgap while it influences the PLQY.[38] These studies underline that surface adsorbed species such as metal cations have little influence on the QD bandgap. To support this hypothesis, one can refer to the XPS analysis of Ramasamy *et al*. on similar InP QDs samples.[20] These authors observed two P 2p features separated by an 0.8 eV shift in unoxidized InP QDs. Such a shift is close to what has been measured between crystalline and amorphous InP films.[39] We hypothesize that the amorphous peak can come from the surface species. The impact of such an amorphous highly disordered external layer on the QDs electronic should not be the same as a pure crystalline layer.[39] Therefore the oxidation of this external layer does not affect the charge carrier confinement, the latter being mostly dependent of the crystalline InP size.

	Zn precursor	Oxidation (%)	P.L. max. (nm)	PLQY (%)	FWHM (nm)
InP/ZnS	$ZnCl_2$	<3	623	4	50
	$Zn(RCOO)_2$	51	616	15	59
		60	625	38	62
InP/ZnSe	$ZnCl_2$	<2	616	12	48
	$Zn(RCOO)_2$	58	609	25	52

Table 1: Structural and optical properties of different samples.

This work also enables us to address the relation between the composition of the core/shell interface and the optical properties of InP-based QDs. As summarized in Table 1, samples with on oxidized core/shell interface systematically feature a higher PLQY than samples with an oxide-free interface. Hence, interfacial oxide appears beneficial for the PLQY. This relation could explain why a high PLQY has been observed in green emitting $(TMS)_3P$-based InP QDs,[11] for which an oxidized interface has been reported.[14] It is also consistent with the beneficial effect of water in the aminophosphine-based InP QDs synthesis that produces green-emitting oxidized InP/ZnS QDs with a higher PLQY than the red-emitting less-oxidized InP/ZnS QDs.[20] As mentioned before, InP/ZnS or InP/ZnSe QDs are both III-V/II-VI heterostructures. As indicated by the low PLQY of the oxide free InP/ZnS and InP/ZnSe QDs, such heterostructures may have an inherently defective interface. Possibly, the interfacial oxide acts as a buffer layer that passivates such interface defects. In spite of its beneficial effect on the PLQY, an oxide may not be the best possible intermediate layer between the core and the shell. Indeed, as can be seen here and in the literature, it seems difficult to attain a PLQY higher than 50 % through interfacial oxidation. Moreover, as can be seen in Table 1, interfacial oxidation broadens the emission line. Possibly, this reflects the chemical heterogeneity of the interfacial oxide, as attested by the FBCP and HETCOR NMR spectra.

Conclusion. This study shows that the nature and the quality of the interface layer of InP-based core/shell QDs are key parameters and, they require to be controlled in order to optimize their photoluminescence properties. We have demonstrated that via the aminophosphine-based InP QDs synthesis we can obtain oxide-free nanomaterial. However in the case of oxide-free core/shell InP QDs, the pure III-V to II-VI junction results in interface defects. We have shown that InP/ZnS and InP/ZnSe QDs with the highest PLQY are obtained when an oxidation layer is present at the core/shell interface. This oxide interface plays the role of buffer layer mitigating the III/V II/VI mismatch. However, this beneficial effect is limited (detrimental influence on the FWHM) in particular because this is a zone in which several defects are incorporated. Other materials presenting a better compatibility with InP in terms of lattice mismatch and band alignment has to be sought. In this sense, an interesting potential candidate is GaP which has shown to improve the InP-based core/shell QDs emission properties.[12,40] This work, thus, paves the way for designing a new generation of highly performing QDs including materials at the interface of InP core and Zn-based shell but also oxide-free material in order to avoid oxide-derived dangling bonds.

ASSOCIATED CONTENT

Supporting Information

The Supporting Information is available free of charge on the ACS Publications website. Experimental Section, TEM, and solid state NMR data of InP QDs, the ZnS-coated, and ZnSe-coated versions.

AUTHOR INFORMATION

Corresponding Authors

*E-mail: mickael.tessier@ugent.be (M.T.), fdelpech@insatoulouse.fr (F.D.) and zeger.hens@ugent.be (Z.H.).

Author Contributions

‡These authors contributed equally to this work.

Notes

The authors declare no competing financial interests.

ACKNOWLEDGMENT

We thank L. Biadala and C. Delerue for fruitful discussion. Z.H. acknowledges support by the European Commission via the Marie-Sklodowska Curie action Phonsi (H2020-MSCA-ITN-642656), by the Research Foundation Flanders (project 17006602) and by Ghent University (GOA no. 01G01513). Z.H., M.T. and D.D. acknowledge the Strategisch Initiatief Materialen in Vlaanderen of Agentschap Innoveren en Ondernemen (SIM VLAIO)." vzw (SBO-QDOCCO, ICON-QUALIDI). This work was supported by the Université Paul Sabatier, the Région Midi-Pyrénées, the CNRS, the Institut National des Sciences Appliquées of Toulouse and the Agence Nationale pour la

Recherche (Project ANR-13-IS10-0004-01). E. A. B. is grateful to Marie Curie Actions and Campus France for a PRESTIGE post-doc fellowship (FP7/2007–2013) under REA grant agreement no. PCOFUND-GA-2013-609102. E.B. acknowledges financial support from the Research Foundation Flanders (FWO, Belgium).

REFERENCES

(1) Kovalenko, M. V; Manna, L.; Cabot, A.; Hens, Z.; Talapin, D. V; Kagan, C. R.; Klimov, X. V. I.; Rogach, A. L.; Reiss, P.; Milliron, D. J.; et al. Prospects of Nanoscience with Nanocrystals. *ACS Nano* **2015**, *9*, 1012–1057.

(2) Bourzac, K. Quantum Dots Go on Display. *Nature* **2013**, *493*, 283.

(3) Tamang, S.; Lincheneau, C.; Hermans, Y.; Jeong, S.; Reiss, P. Chemistry of InP Nanocrystal Syntheses. *Chem. Mater.* **2016**, *28*, 2491–2506.

(4) Song, W.-S.; Lee, H.-S.; Lee, J. C.; Jang, D. S.; Choi, Y.; Choi, M.; Yang, H. Amine-Derived Synthetic Approach to Color-Tunable InP/ZnS Quantum Dots with High Fluorescent Qualities. *J. Nanoparticle Res.* **2013**, *15*, 1750.

(5) Tessier, M. D.; Dupont, D.; De Nolf, K.; De Roo, J.; Hens, Z. Economic and Size-Tunable Synthesis of InP/ZnE (E = S,Se) Colloidal Quantum Dots. *Chem. Mater.* **2015**, *27*, 4893–4898.

(6) Kim, K.; Yoo, D.; Choi, H.; Tamang, S.; Ko, J.-H.; Kim, S.; Kim, Y.-H.; Jeong, S. Halide-Amine Co-Passivated Indium Phosphide Colloidal Quantum Dots in Tetrahedral Shape. *Angew. Chemie Int. Ed.* **2016**, *55*, 3714 –3718.

(7) Tessier, M. D.; De Nolf, K.; Dupont, D.; Sinnaeve, D.; De Roo, J.; Hens, Z. Aminophosphines: A Double Role in the Synthesis of Colloidal Indium Phosphide Quantum Dots. *J. Am. Chem. Soc.* **2016**, *138*, 5923–5929.

(8) Panzer, R.; Guhrenz, C.; Haubold, D.; Hübner, R.; Gaponik, N.; Eychmüller, A.; Weigand, J. J. Versatile Tri(Pyrazolyl)Phosphanes as Phosphorus Precursors for the Synthesis of Highly Emitting InP/ZnS Quantum Dots. *Angew. Chemie - Int. Ed.* **2017**, *56*, 14737–14742.

(9) Chen, O.; Zhao, J.; Chauhan, V. P.; Cui, J.; Wong, C.; Harris, D. K.; Wei, H.; Han, H.-S.; Fukumura, D.; Jain, R. K.; et al. Compact High-Quality CdSe-CdS Core-Shell Nanocrystals with Narrow Emission Linewidths and Suppressed Blinking. *Nat. Mater.* **2013**, *12*, 445–451.

(10) Pu, C.; Peng, X. To Battle Surface Traps on CdSe/CdS Core/Shell Nanocrystals: Shell Isolation versus Surface Treatment. *J. Am. Chem. Soc.* **2016**, *138*, 8134–8142.

(11) Li, L.; Reiss, P. One-Pot Synthesis of Highly Luminescent InP / ZnS Nanocrystals Without. *J. Am. Chem. Soc.* **2008**, *130*, 11588–11589.

(12) Pietra, F.; Kirkwood, N.; De Trizio, L.; Hoekstra, A. W.; Kleibergen, L.; Renaud, N.; Koole, R.; Baesjou, P.; Manna, L.; Houtepen, A. J. Ga for Zn Cation Exchange Allows for Highly Luminescent and Photostable InZnP-Based Quantum Dots. *Chem. Mater.* **2017**, *29*, 5192–5199.

(13) Ramasamy, P.; Kim, N.; Kang, Y. S.; Ramirez, O.; Lee, J. S. Tunable, Bright, and Narrow-Band Luminescence from Colloidal Indium Phosphide Quantum Dots. *Chem. Mater.* **2017**, *29*, 6893–6899.

(14) Cros-Gagneux, A.; Delpech, F.; Nayral, C.; Cornejo, A.; Coppel, Y.; Chaudret, B. Surface Chemistry of InP Quantum Dots: A Comprehensive Study. *J. Am. Chem. Soc.* **2010**, *132*, 18147–18157.

(15) Micic, O. I.; Sprague, J. R.; Curtis, C. J.; Jones, K. M.; Machol, J. L.; Nozik, A. J.; Giessen, H.; Fluegel, B.; Mohs, G.; Peyghambarian, N. Synthesis and Characterization of InP , Gap , and GaInP2 Quantum Dots. *J. Phys. Chem.* **1995**, *99*, 7754–7759.

(16) Battaglia, D.; Peng, X. Formation of High Quality InP and InAs Nanocrystals in a Noncoordinating Solvent. *Nano Lett.* **2002**, *2*, 1027–1030.

(17) Xie, R.; Battaglia, D.; Peng, X. Colloidal InP Nanocrystals as Efficient Emitters Covering Blue to Near-Infrared. *J. Am. Chem. Soc.* **2007**, *129*, 15432–15433.

(18) Baquero, E. A.; Virieux, H.; Swain, R. A.; Gillet, A.; Cros-Gagneux, A.; Coppel, Y.; Chaudret, B.; Nayral, C.; Delpech, F. Synthesis of Oxide-Free InP Quantum Dots: Surface Control and H2-Assisted Growth. *Chem. Mater.* **2017**, *29*, 9623–9627.

(19) Xie, L.; Harris, D. K.; Bawendi, M. G.; Jensen, K. F. Effect of Trace Water on the Growth of Indium Phosphide Quantum Dots. *Chem. Mater.* **2015**, *27*, 5058–5063.

(20) Ramasamy, P.; Kim, B.; Lee, M.-S.; Lee, J.-S. Beneficial Effects of Water in the Colloidal Synthesis of InP/ZnS Core–shell Quantum Dots for Optoelectronic Applications. *Nanoscale* **2016**, *8*, 17159–17168.

(21) Buffard, A.; Dreyfuss, S.; Nadal, B.; Heuclin, H.; Xu, X.; Patriarche, G.; Mézailles, N.; Dubertret, B. Mechanistic Insight and Optimization of InP Nanocrystals Synthesized with Aminophosphines. *Chem. Mater.* **2016**, *28*, 5925–5934.

(22) Baquero, E. A.; Ojo, W.-S.; Coppel, Y.; Chaudret, B.; Urbaszek, B.; Nayral, C.; Delpech, F. Identifying Short Surface Ligands on Metal Phosphide Quantum Dots. *Phys. Chem. Chem. Phys.* **2016**, *18*, 17330–17334.

(23) Hens, Z.; Martins, J. C. A Solution NMR Toolbox for Characterizing the Surface Chemistry of Colloidal Nanocrystals. *Chem. Mater.* **2013**, *25*, 1211–1221.

(24) Rafipoor, M.; Dupont, D.; Tornatzky, H.; Tessier, M. D.; Maultzsch, J.; Hens, Z.; Lange, H. Strain Engineering in InP/(Zn,Cd)Se Core/Shell Quantum Dots. *Chem. Mater.* **2018**, *30*, 4393–4400.

(25) Sluydts, M.; De Nolf, K.; Van Speybroeck, V.; Cottenier, S.; Hens, Z. Ligand Addition Energies and the Stoichiometry of Colloidal Nanocrystals. *ACS Nano* **2016**, *10*, 1462–1474.

(26) Cossairt, B. M.; Stein, J. L.; Holden, W. M.; Seidler, G. T. Role of Phosphorus Oxidation in Controlling the Luminescent Properties of Indium Phosphide Quantum Dots. *SID Symp. Dig. Tech. Pap. [0097-966X]* **2018**, *49*, 21–24.

(27) Kley, A.; Neugebauer, J. Atomic and Electronic Structure of the GaAs/ZnSe(001) Interface. *Phys. Rev. B* **1994**, *50*, 8616–8628.

(28) Deng, H. X.; Luo, J. W.; Wei, S. H. Chemical Trends of Stability and Band Alignment of Lattice-Matched II-VI/III-V Semiconductor Interfaces. *Phys. Rev. B - Condens. Matter Mater. Phys.* **2015**, *91*, 075315.

(29) Stroppa, A.; Peressi, M. ZnSe GaAs(001) Heterostructures with Defected Interfaces: Structural, Thermodynamic, and Electronic Properties. *Phys. Rev. B - Condens. Matter Mater. Phys.* **2005**, *72* , 245304.

(30) El-Brolossy, T. A.; Abdalla, S.; Negm, S.; Talaat, H. Interfacial Electronic Traps at ZnSe/GaAs Heterostructures Studied by Photomodulation Raman Scattering. *J. Phys. Condens. Matter* **2006**, *18*, 4189–4195.

(31) Yesinowski, J. P.; Eckert, H. Hydrogen Environments in Calcium Phosphates: H MAS NMR at High Spinning Speeds. *J. Am. Chem. Soc.* **1987**, *109*, 6274–6282.

(32) Arends, J.; Christoffersen, J.; Christoffersen, M. R.; Eckert, H.; Fowler, B. O.; Heughebaert, J. C.; Nancollas, G. H.; Yesinowski, J. P.; Zawacki, S. J. A Calcium Hydroxyapatite Precipitated from an Aqueous Solution. An International Multimethod Analysis. *J. Cryst. Growth* **1987**, *84*, 515–532.

(33) Peng, X. An Essay on Synthetic Chemistry of Colloidal Nanocrystals. *Nano Res.* **2009**, *2*, 425–447.

(34) Virieux, H.; Le Troedec, M.; Cros-Gagneux, A.; Ojo, W. S.; Delpech, F.; Nayral, C.; Martinez, H.; Chaudret, B. InP/ZnS Nanocrystals: Coupling NMR and XPS for Fine Surface and Interface Description. *J. Am. Chem. Soc.* **2012**, *134*, 19701–19708.

(35) Tomaselli, M.; Yarger, J. L.; Bruchez, M.; Havlin, R. H.; De Graw, D.; Pines, A.; Alivisatos, A. P. NMR Study of InP Quantum Dots: Surface Structure and Size Effects. *J. Chem. Phys.* **1999**, *110*, 8861–8864.

(36) Deng, Z.; Jeong, K. S.; Guyot-Sionnest, P. Colloidal Quantum Dots Intraband Photodetectors. *ACS Nano* **2014**, *8*, 11707–11714.

(37) Sagar, L. K.; Walravens, W.; Maes, J.; Geiregat, P.; Hens, Z. HgSe/CdE (E = S, Se) Core/Shell Nanocrystals by Colloidal Atomic Layer Deposition. *J. Phys. Chem. C* **2017**, *121*, 13816–13822.

(38) Zhang, Y.; Zhang, Z.; Yin, D.; Li, J.; Xie, R.; Yang, W. Turn-on Fluorescent InP Nanoprobe for Detection of Cadmium Ions with High Selectivity and Sensitivity. *ACS Appl. Mater. Interfaces*

2013, *5*, 9709–9713.

(39) Theye, M. L.; Gheorghiu, A.; Udron, D.; Senemaud, C.; Belin, E.; Von Bardeleben, J.; Squelard, S.; Dupin, J. Defect States in Amorphous InP. *J. Non. Cryst. Solids* **1987**, *97–98* (part 2), 1107–1110.

(40) Kim, S.; Kim, T.; Kang, M.; Kwak, S. K.; Yoo, T. W.; Park, L. S.; Yang, I.; Hwang, S.; Lee, J. E.; Kim, S. K.; et al. Highly Luminescent InP/GaP/ZnS Nanocrystals and Their Application to White Light-Emitting Diodes. *J. Am. Chem. Soc.* **2012**, *134*, 3804–3809.

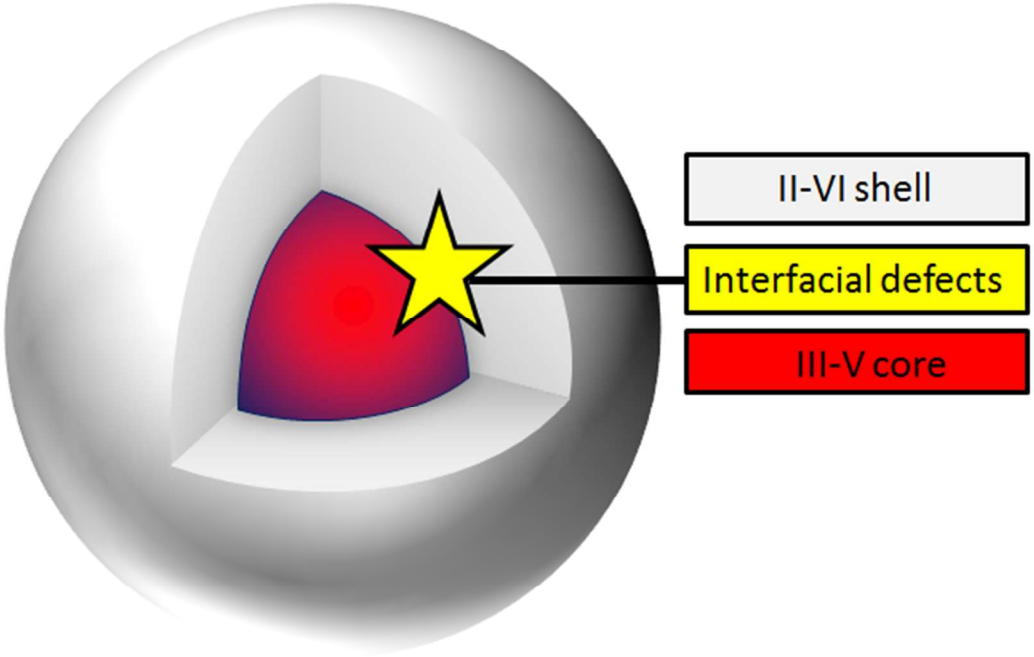
II-VI shell
Interfacial defects
III-V core